

therefore apply also to  $P_p$ .

<sup>10</sup>In view of the Basel convention we have chosen the  $x$ ,  $y$ , and  $z$  axes as coinciding with  $-x'$ ,  $y'$ , and  $-z'$  axes, respectively, of Verhaar and Tolsma, Ref. 8.

<sup>11</sup>A. Dar, Phys. Letters 7, 339 (1963).

<sup>12</sup>For this reason we have preferred in this paper to indicate our model as "generalized ring-locus model,"

instead of "finite-angular-width ring-locus model," as it was introduced in Ref. 8. Whereas the finite angular width of the ring locus is the feature primarily responsible for the reverse-rotation phenomenon in inelastic  $\alpha$ -particle scattering, its displacement relative to the bisector plane seems to be of special importance for the polarization effects discussed here.

### NEW NUCLIDES $^{19}\text{Na}$ AND $^{23}\text{Al}$ OBSERVED VIA THE $(p, {}^6\text{He})$ REACTION\*

Joseph Cerny, R. A. Mendelson, Jr., G. J. Wozniak, John E. Esterl, and J. C. Hardy

Department of Chemistry and Lawrence Radiation Laboratory,

University of California, Berkeley, California 94720

(Received 3 February 1969)

By employing the reactions  $^{24}\text{Mg}(p, {}^6\text{He})^{19}\text{Na}$  and  $^{28}\text{Si}(p, {}^6\text{He})^{23}\text{Al}$  [ $d\sigma/d\Omega \sim 100$  nb/sr], the mass excesses of  $^{19}\text{Na}$  and  $^{23}\text{Al}$  are found to be  $12.974 \pm 0.070$  and  $6.766 \pm 0.080$  MeV, respectively [ $^{12}\text{C} = 0$ ]. Since  $^{19}\text{Na}$  is determined to be proton unstable,  $^{23}\text{Al}$  should be the lightest, nucleon-stable member of the  $A = 4n + 3$ ,  $T_Z = -\frac{3}{2}$  mass series.

Although the masses and decay schemes of the  $A = 4n + 1$  series of  $T_Z = -\frac{3}{2}$  nuclei in the light elements are fairly well established,<sup>1</sup> almost nothing is known about the comparable  $4n + 3$  nuclei. Only the properties of  ${}^7\text{B}$  in the latter series are known<sup>2</sup> and only  ${}^{11}\text{N}$  can be additionally studied using existing nuclear-reaction techniques and stable targets. We wish herein to report the successful utilization of a new nuclear-reaction tool—the  $(p, {}^6\text{He})$  reaction—capable of studying in general these  $4n + 3$ ,  $T_Z = -\frac{3}{2}$  nuclei. The masses of  $^{19}\text{Na}$  and  $^{23}\text{Al}$  have been measured via the reactions  $^{24}\text{Mg}(p, {}^6\text{He})^{19}\text{Na}$  and  $^{28}\text{Si}(p, {}^6\text{He})^{23}\text{Al}$ ; these masses agree well with various mass predictions.

Preliminary measurements had shown that the  $(p, {}^6\text{He})$  reaction producing such  $4n + 3$  nuclei ( $Q \sim -37$  MeV) possessed a differential cross section of  $\sim 100$  nb/sr; so techniques capable of observing such small yields had to be employed. Our basic approach has been described previously<sup>3</sup> so that only the improvements to this system will be detailed here.

A 54.7-MeV proton beam from the Berkeley 88-in. cyclotron was used to bombard thin targets of adenine ( $\text{C}_5\text{H}_5\text{N}_5$ ),  $^{24}\text{Mg}$ , and natural silicon. Reactions occurring on the first target provided calibration groups. Figure 1 presents a diagram of one of the two similar counter-telescope and electronic systems which were simultaneously employed; the counter telescopes were placed at  $14.1^\circ$  on opposite sides of the beam. Four silicon transmission detectors were used in each telescope. After a fast coincidence

among the first three detectors restricted the origin of all allowed events to a single beam burst, two particle identifications (PI) were performed and compared using the signals from the two successive differential-energy-loss detectors—denoted as  $\Delta E2$  and  $\Delta E1$ , respectively—and the third "E" detector.<sup>3</sup> Any events traversing the first three counters were rejected by the fourth.

Even with the above electronics, pile-up between events coincident within a single beam burst creates a substantial background ( $\sim 50$  nb/sr at our typical counting rate) and interferes with or prevents studies of unusual nuclear reactions with cross sections below 100 nb/sr. As a result, time-of-flight (TOF) measurements over the 51-cm flight path between the target and the  $\Delta E2$  counter have been added; a resulting mass calculation readily distinguishes true  ${}^6\text{He}$  events from ones arising, for example, from  ${}^3\text{He}-d$  pile-up that also appear in the  ${}^6\text{He}$  region of the PI spectrum.<sup>3</sup> In addition, a subnanosecond pile-up detection system (PUD) on the signal from the  $\Delta E2$  counter places a further requirement on each event. These improvements drastically reduce the chance coincidence background and would appear to make feasible the study of highly endothermic nuclear reactions with cross sections as low as 10 nb/sr.

An outline of the added TOF and PUD electronics is also shown in Fig. 1. A timing pulse was obtained from the first ( $\Delta E2$ ) detector via a fast charge-sensitive preamplifier (10–90% rise time of 4 nsec for zero capacitance). For these purposes, signals from this preamplifier were used

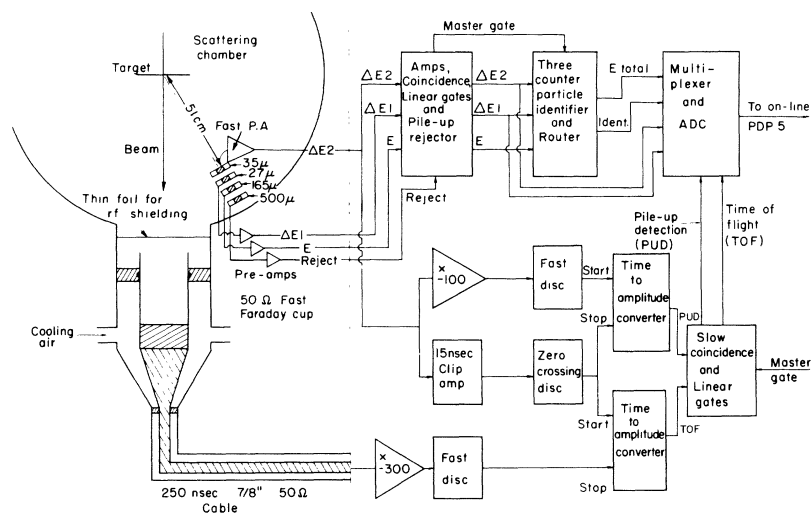


FIG. 1. An abbreviated diagram of the experimental layout and the electronic equipment for one of the two similar detection systems employed in these measurements.

in two ways. First, utilizing the leading edge of the pulse, they provided a start signal for the PUD system time-to-amplitude converter. Second, by clipping this tail pulse to form a bipolar pulse of 30-nsec total width, a timing signal was obtained from the zero-crossing point. This latter pulse provided the PUD stop pulse for the time-to-amplitude converter (also see below). Any deviation between the normal leading-edge and crossover time was indicative of pile-up. A resolution of 0.2 nsec for 10-MeV energy loss in the  $\Delta E2$  counter was obtainable with a maximum walk of 0.3 nsec for pulses between 1.5 and 10 MeV.

The zero-crossing discriminator output was also used to start another time-to-amplitude converter which was stopped by a pulse derived from the arrival time of a beam burst in the fast Faraday cup shown in Fig. 1. Because of the fairly low-frequency, sector-focused design of the Berkeley cyclotron—which normally provides a  $45^\circ$  phase width [full width at half-maximum (FWHM)] at 15.9 MHz for the 54.7-MeV proton beam—it was necessary to restrict the phase width to about  $6^\circ$  by the use of internal collimators. Even with these collimators, however, it was possible to obtain energy-analyzed beam (0.14%) with intensities of  $2.5 \mu\text{A}$ . An overall time resolution of 1.4-nsec FWHM was measured.

Events in each system with acceptable identifications were sent via an analog-to-digital converter, multiplexer system to an on-line PDP-5 computer. Six parameters— $\Delta E2$ ,  $\Delta E1$ ,  $E_T(\text{total})$ ,

PI, TOF, and PUD—were recorded for each event. The computer also stored 20 pulser-simulated  $^6\text{He}$  events every hour to check both electronic systems and provide an accurate measure of drifts. A monitor counter independently measured the beam-energy variation with time. Following the run, each  $^6\text{He}$  event was analyzed in detail. The PUD was corrected for time walk of the leading-edge trigger, and mass information was obtained by calculating  $E_T(\text{TOF})^2$ ; the latter yielded an overall FWHM of 0.6 amu for mass six. “Windows” were set on the PI, PUD, and mass data.

Figure 2 presents final energy spectra from the reactions  $^{12}\text{C}(p, ^6\text{He})^7\text{B}$ ,  $^{14}\text{N}(p, ^6\text{He})^9\text{C}$ ,  $^{24}\text{Mg}(p, ^6\text{He})^{19}\text{Na}$ , and  $^{28}\text{Si}(p, ^6\text{He})^{23}\text{Al}$ . The  $^{14}\text{N}(p, ^6\text{He})^9\text{C}$  data were used for calibration purposes. Runs of 2- to 5-h duration on the adenine target were interspersed with longer runs on the other targets to minimize any effects due to beam instability. Only data from System 2 are shown for the adenine and  $^{24}\text{Mg}$  targets; the cross sections for production of  $^9\text{C}$  and  $^{19}\text{Na}$  are  $\sim 160$  and  $\sim 120$  nb/sr, respectively. Results from both systems are combined for the  $^{23}\text{Al}$  data because the target was thinner and the cross section about a factor of 3 lower. The spectra appear quite clean after the mass and pile-up restrictions have been applied, with the slightly greater background at the higher energies in the silicon spectrum probably arising from reactions on  $^{29}\text{Si}$  and  $^{30}\text{Si}$ . If the adenine data were considered without these mass and pile-up restrictions, for example, the energy re-

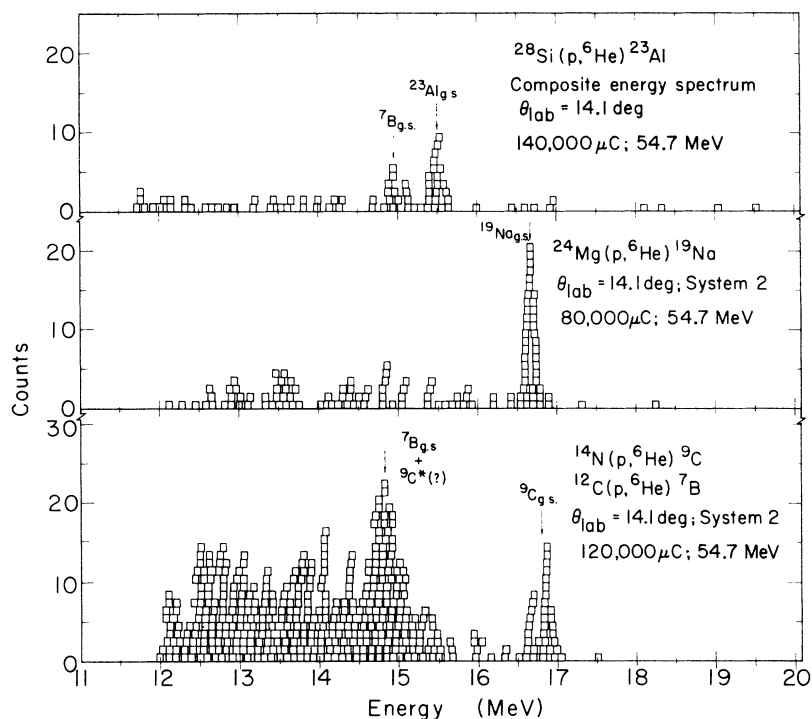


FIG. 2. The energy spectra from the  $(p, {}^6\text{He})$  reaction on adenine (bottom),  ${}^{24}\text{Mg}$  (middle), and natural silicon (top). Data from detection System 2 only are shown for the last two targets, while data from both systems are combined to produce the spectrum for  ${}^{28}\text{Si}(p, {}^6\text{He}){}^{23}\text{Al}$ . Each block is one count and the block width is 80 keV. Transitions to the first excited state of  ${}^9\text{C}$  might be present, distorting the spectrum of the  ${}^7\text{B}$  ground state in the data from the adenine target.

gion of interest would contain a continuous background of magnitude  $\sim\frac{1}{3}$  the corrected  ${}^9\text{C}$  ground-state peak extending from the  ${}^7\text{B}$  ground state to  $\sim 18$  MeV as well as scattered counts at higher energies. The ground-state transitions for  ${}^9\text{C}$ ,  ${}^{19}\text{Na}$ , and  ${}^{23}\text{Al}$  all have widths consistent with the expected energy resolution.

The mass excess of  ${}^{19}\text{Na}$  is determined to be  $12.974 \pm 0.070$  MeV [ ${}^{12}\text{C} = 0$ ]. Since the first excited state in the  $T = \frac{3}{2}$ ,  $T_Z = \frac{1}{2}(N-Z) = \frac{3}{2}$  analog nucleus  ${}^{19}\text{O}$  lies at only 96-keV excitation<sup>4</sup> (the next state is at 1.47 MeV) and since the mechanism of the  $(p, {}^6\text{He})$  reaction is uncertain, there is some ambiguity as to whether this mass excess applies

to the ground state and/or to the first excited state of  ${}^{19}\text{Na}$  (the experimental resolution was  $\sim 200$  keV). We will take it to be the ground state noting that in either event  ${}^{19}\text{Na}$  is proton unstable; with this assumption,  ${}^{19}\text{Na}$  is unbound to  ${}^{18}\text{Ne} + p$  by  $366 \pm 70$  keV.

The mass excess of  ${}^{23}\text{Al}$  is determined to be  $6.766 \pm 0.080$  MeV. (The data in Fig. 2 also show the presence of  ${}^7\text{B}$  ground state from reactions on a  ${}^{12}\text{C}$  target impurity.<sup>5</sup>) Therefore,  ${}^{23}\text{Al}$  is bound to  ${}^{22}\text{Mg} + p$  by  $146 \pm 82$  keV<sup>6</sup> and is nucleon stable. It should be the lightest such isotope in the  $T_Z = -\frac{3}{2}$ ,  $4n + 3$  mass series, is expected to have a half-life  $< 600$  msec, and should emit  $\beta$ -delayed

Table I. Experimental and predicted mass excesses (in MeV  $\pm$  keV).

Nuclide	Mass	IMME <sup>a</sup>	Predictions $d_{5/2}$ shell Coulomb <sup>b</sup>	Kelson-Garvey <sup>c</sup>
${}^{19}\text{Na}$	$12.974 \pm 70$	$12.90 \pm 130$	$12.965 \pm 25$	12.87
${}^{23}\text{Al}$	$6.766 \pm 80$	$6.766 \pm 98$	$6.743 \pm 25$	6.71

<sup>a</sup>Cerny, Ref. 1.

<sup>b</sup>Hardy, Brunnader, Cerny, and Jänecke, Ref. 9.

<sup>c</sup>Kelson and Garvey, Ref. 10.

protons of  $\sim 200$  keV. Only the ground state of  $^{23}\text{Al}$  is likely to be bound, since the first excited state of the analog nucleus  $^{23}\text{Ne}$  lies at 1.02 MeV.<sup>7</sup>

Both of these nuclei complete isobaric quartets<sup>8,9</sup>; their masses have already been predicted by the isobaric multiplet mass equation (IMME), as discussed in Ref. 1, and thus permit yet another check of its validity. Mass predictions for these nuclei from the IMME,<sup>1</sup> from a systematic study of Coulomb energies in the  $1d_{5/2}$  shell,<sup>9</sup> and from the Kelson-Garvey nuclidic mass relationship<sup>10</sup> are given in Table I. Good agreement is to be seen among the various theoretical predictions and between them and experiment for both  $^{19}\text{Na}$  and  $^{23}\text{Al}$ .

We would like to thank Dr. Jurgen Radloff for developing the fast preamplifier used in these experiments, Dr. Francesco Resmini and Dr. David Clark for their efforts in preparing beams with suitable phase widths, Barbara Cerny for writing the off-line analysis program, and John Bowen and the cyclotron crew for maintaining the beam throughout a long, arduous run.

\*Work performed under the auspices of the U. S. Atomic Energy Commission.

<sup>1</sup>J. Cerny, *Ann. Rev. Nucl. Sci.* **18**, 27 (1968).

<sup>2</sup>R. L. McGrath, J. Cerny, and E. Norbeck, *Phys. Rev. Letters* **19**, 1442 (1967).

<sup>3</sup>G. W. Butler, J. Cerny, S. W. Cosper, and R. L. McGrath, *Phys. Rev.* **166**, 1096 (1968).

<sup>4</sup>J. L. Wiza and R. Middleton, *Phys. Rev.* **143**, 676 (1966).

<sup>5</sup>Very tentative evidence for the reaction  $^{16}\text{O}(p, ^6\text{He})^{11}\text{N}$  on oxygen target impurities was noted; however, this transition could not interfere with the ground-state measurements.

<sup>6</sup>The  $^{22}\text{Mg}$  mass is taken to be  $-377 \pm 16$  keV as a weighted average of the values reported in J. Cerny, S. W. Cosper, G. W. Butler, R. H. Pehl, F. S. Goulding, D. A. Landis, and C. Détraz, *Phys. Rev. Letters* **16**, 469 (1966); P. H. Barker, N. Drysdale, and W. R. Phillips, *Proc. Phys. Soc. (London)* **91**, 587 (1967); A. B. McDonald and E. G. Adelberger, *Bull. Am. Phys. Soc.* **12**, 1145 (1967); J. M. Adams, A. Adams, and J. M. Calvert, *J. Phys. A: Phys. Soc. (London) Proc.* **1**, 549 (1968).

<sup>7</sup>A. J. Howard, J. P. Allen, D. A. Bromley, J. W. Olness, and E. K. Warburton, *Phys. Rev.* **154**, 1067 (1967).

<sup>8</sup>In fact, as is discussed in Refs. 1 and 9, the mass 19 isobaric multiplet for which three members are known comprises the first excited  $T = \frac{3}{2}$  states ( $J^\pi = \frac{3}{2}^+$ ) in the  $T_Z = \frac{3}{2}$ ,  $\frac{1}{2}$ , and  $-\frac{1}{2}$  nuclei.

<sup>9</sup>J. C. Hardy, H. Brunnader, J. Cerny, and J. Jä-necke, to be published.

<sup>10</sup>I. Kelson and G. T. Garvey, *Phys. Letters* **23**, 689 (1966).

### THE DECAY $\Sigma^\pm \rightarrow \Lambda e^\pm \nu$

C. Baltay,\* P. Franzini, R. Newman, H. Norton, and N. Yeh

Columbia University, New York, New York 10027, and Brookhaven National Laboratory, Upton, New York 11973

and

J. Cole, J. Lee-Franzini, R. Loveless, and J. McFadyen

State University of New York, Stony Brook, New York 11790,  
and Brookhaven National Laboratory, Upton, New York 11973

(Received 20 February 1969)

We have observed 46 examples of the decay  $\Sigma^- \rightarrow \Lambda e^- \nu$  and six of the decay  $\Sigma^+ \rightarrow \Lambda e^+ \nu$ . The branching ratios are, respectively,  $(0.52 \pm 0.09) \times 10^{-4}$  and  $(0.16 \pm 0.07) \times 10^{-4}$ . A study of the internal variables distribution yields  $G_V/G_A = -0.7 \pm 0.4$  for the combined sample of  $\Sigma^\pm \rightarrow \Lambda e^\pm \nu$ .

The decays  $\Sigma^\pm \rightarrow \Lambda e^\pm \nu$  offer one of the rare instances in which it is possible to measure a matrix element of the strangeness-conserving weak current between baryon states. Lorentz invariance and the absence of second-class currents imply that the matrix element in question may be written as<sup>1</sup>

$$\langle \Lambda | J_\mu^{\Delta S=0} | \Sigma \rangle = \bar{u}_\Lambda \{ G_V \gamma_\mu + (G_{\text{wk}}/M) \sigma_{\mu\nu} q_\nu + G_A \gamma_\mu \gamma_5 + (G_{\text{ps}}/M) q_\mu \gamma_5 \} u_\Sigma. \quad (1)$$

The complete amplitude for  $\Sigma^- \rightarrow \Lambda e^- \nu$  decay is given by

$$\mathfrak{M} = \langle \Lambda | J_\mu | \Sigma \rangle \bar{u}_e \gamma_\mu (1 + \gamma_5) u_\nu. \quad (2)$$